ANTIOXIDANTS & REDOX SIGNALING
Volume 19, Number 5, 2013

DOI: 10.1089/ars.2012.4563

Therapeutics

ORIGINAL RESEARCH COMMUNICATION

# Targeting Nitric Oxide Signaling with nNOS Inhibitors As a Novel Strategy for the Therapy and Prevention of Human Melanoma

Zhen Yang,[1,2] Bobbye Misner,[1] Haitao Ji,[3] Thomas L. Poulos,[4–6] Richard B. Silverman,[3] Frank L. Meyskens,[1,7–9] and Sun Yang[1,4,7]

## Abstract

***Aims:*** Our previous studies have shown that nitric oxide (NO) plays an important role in increasing the invasion and proliferation of human melanoma cells, suggesting that targeting NO signaling may facilitate therapy and prevention. Neuronal nitric oxide synthase (nNOS) is present in melanocytes, a cell type that originates from the neural crest. The aims of this study were to determine the role of nNOS in melanoma progression and the potential antitumor effects of novel synthesized nNOS inhibitors. ***Results:*** *In vitro* studies demonstrated abundant expression of nNOS in melanoma compared to melanocytes, which was inducible by ultraviolet radiation and was associated with increased NO generation. nNOS was also detected in melanoma biopsies that increased with disease stage. Knockdown of nNOS in melanoma cells diminished L-arginine-induced NO production; the metastatic capacity was also reduced as well as the levels of MMP-1, Bcl-2, JunD, and APE/Ref-1. Similar inhibition of NO and invasion potential was observed utilizing novel, highly selective nNOS inhibitors. In three-dimensional human skin reconstructs, the nNOS inhibitor cpd8 effectively reversed the melanoma overgrowth stimulated by NO stress. ***Innovation:*** Our work lays the foundation for development of clinical "drug-like" nNOS inhibitors as a new and promising strategy for the chemoprevention of early melanoma progression and the inhibition of secondary melanoma in high-risk individuals. ***Conclusion:*** Based on our observations, we propose that nNOS in melanoma results in constitutive overproduction of NO, which stimulates proliferation and increases invasion potential, leading to subsequent development of metastases. *Antioxid. Redox Signal.* 19, 433–447.

## Introduction

Ultraviolet (UV) radiation has been implicated as a major environmental contributor to the development of most cutaneous melanomas (CMs). Sunscreens and sun awareness behavior have been used for the prevention of CM, but their clinical utility remains controversial (6). The mechanistic role of UV radiation in melanomagenesis needs to be more comprehensively defined (39,40). In human skin, UV radiation not only generates reactive oxygen species (ROS), but also produces a marked increase of nitric oxide (NO) (48). The contributions of ROS to melanomagenesis have been extensively studied by our group and other researchers; however, characterizations of the effects of NO and its detailed molecular mechanisms have been quite limited. NO is predominantly produced from L-arginine by nitric oxide synthase (NOS). *Via* interacting with superoxide anion, NO generates highly reactive oxidants such as peroxynitrite, resulting in DNA damage and protein modifications at the post-transcriptional levels, including S-nitrosylation and S-glutathionylation (34). These biochemical changes are associated with carcinogenesis, cell cycle progression, drug resistance, and antiapoptosis (38,44,45,54,55). In the skin, serving as an important second messenger, NO-mediated signaling also contributes to UV-induced melanogenesis and pigmentation (47). Large quantities of NO have been detected

[1]Chao Family Comprehensive Cancer Center, University of California Irvine, Irvine, California.
[2]Department of Hepatology, Provincial Hospital, Shandong University, Jinan, China.
[3]Departments of Chemistry and Molecular Biosciences, Chemistry of Life Processes Institute, Center for Molecular Innovation and Drug Discovery, Northwestern University, Evanston, Illinois.
Departments of [4]Pharmaceutical Sciences, [5]Molecular Biology & Biochemistry, [6]Chemistry, [7]Medicine, [8]Biological Chemistry, and [9]Public Health, University of California Irvine, Irvine, California.

**Innovation**

Targeting neuronal nitric oxide synthase/nitric oxide (nNOS/NO) with novel inhibitors represents an innovative strategy for the prevention of melanoma progression. With more selective, bioavailable, and potent inhibitors, we expect to avoid off-target side effects and anticipate that NO/nNOS-targeted therapy will be translated into a clinical compound within the next few years for the chemoprevention and treatment of melanoma. To date, only sunscreens and sun awareness behavior have been proposed or used for the prevention of cutaneous melanoma with mixed results. Our study has also identified that ultraviolet radiation plays a role in cell signaling *via* nNOS–NO pathway relevant to melanoma proliferation and invasion. Our innovative approach targeting nNOS/NO may become highly significant for other malignancies as well.

in many types of cancer tissues, and the roles of NO in carcinogenesis, cell survival and proliferation, tumor growth, and metastasis have been well documented in nonmelanoma skin cancer and other tumors (1,46,48). Constitutive production of NO in melanoma results in increased proliferation, impaired immune response, and lymphangiogenesis, which has been associated with poor survival in patients (13,16,35). However, other studies showed that NO-donating compounds exhibited antimelanoma activities (33). The distinct effects of NO observed might be due to different NO levels and the distinct study models (19,55).

The NOS family comprises the following: inducible (i)NOS, endothelial (e)NOS, and neuronal NOS (nNOS), the latter of which is expressed mainly in neural tissue. Previous studies have largely focused on iNOS and its inhibitors, which exhibited promising chemopreventive activities in skin carcinogenesis but limited antimelanoma potential (8,51). As melanocytes originate from the neural crest and have many gene expression characteristics similar to neural cells (12), nNOS may play a unique role in regulating NO levels in melanocytes. For example, Ahmed *et al.* have reported a progressive increase of nNOS expression in nevi and melanoma biopsy samples (2), suggesting that the *de novo* expression of nNOS may be a marker for an early stage of melanoma. Differential expression of nNOS in tumorigenic and nontumorigenic variants derived from the same melanoma cell line also has been reported (25). In addition, a recent clinical epidemiologic study investigated the role of polymorphisms of nNOS as related to outcome and demonstrated that certain nNOS (but not iNOS) genotypes were associated with an increased risk of CM (28).

In our study, we demonstrate an important role of nNOS in melanoma progression. Utilizing nNOS as a druggable target, we have also synthesized and *in vitro* screened potent specific inhibitors with antimelanoma activities.

## Results

### *NO stress stimulates the proliferation of melanoma cells* in vitro

The NO donor (*Z*)-1-[2-(2-aminoethyl)-*N*-(2-ammonioethyl) amino] diazen-1-ium-1,2-diolate (DETA/NO) was utilized to mimic NO stress in cell culture media. As shown in Figure 1A, in human primary melanocytes, cell proliferation measured by the 3-(4,5-dimethylthiazol-2-yl)-2,5-diphenyltetrazolium bromide colorimetric assay in a 12-day period was significantly stimulated by DETA/NO exposure compared to control. At the end of the experiment, melanocytes incubated with DETA/NO were still proliferating, while the proliferation of control cells peaked by day 6 then decreased. When extending the exposure time of DETA/NO in melanocytes to 10 weeks, surprisingly, we observed that many foci formed in culture dishes and cells exhibited notable vertical growth potential: these foci were subcloned and reseeded at a low density and showed evidence of continued foci formation. Marked stimulation of proliferation was also evident in human metastatic Lu1205 cells with DETA/NO (100 $\mu M$) treatment (Fig. 1B and Supp Fig. S12). Notably, in A375 melanoma cells, as shown in Supplementary Data (Supplementary Fig. S10; Supplementary Data are available online at www.liebertpub.com/ars), such induction by DETA treatment reached a peak at 10 $\mu M$, which was, however, reversed by a higher concentration of DETA (50 $\mu M$), suggesting that a lower level of NO is more proliferative in human melanoma. On the contrary, such increases were not significant in primary melanoma wm3211 cells. The subsequent immunoblotting analysis (Fig. 1E) revealed that DETA treatment only generated a marginal increase of nNOS expression in wm3211 cells, which recovered quickly by 24 h. On the contrary, marked induction of nNOS was evident in metastatic Lu1205 cells and peaked after 24 h of treatment. Such differential regulations of nNOS expression might explain the distinct responses of cells to DETA-stimulated proliferation.

To explore the effects of UV radiation on NO generation, primary melanoma wm3211 cells were irradiated with UVA (3 J/cm$^2$) or UVB (25 mJ/cm$^2$), respectively. The intracellular NO levels were detected by the Griess reagent, which measures nitrite concentrations. Given the fact that nitrate may also be produced in addition to nitrite by NO, such measurement was limited to determine relative NO levels. As shown in Figure 1C and Supplementary Fig. S9, both UVA and UVB significantly induced NO generations; however, the pattern of induction of UVA and UVB was different. UVB-induced NO generation was rapid (30 min), potent, peaked by 4 h, and was gone by 24 h, while the increase of NO by UVA radiation was not evident until after 24 h and lasted for at least 72 h.

Employing the ultrasensitive colorimetric NOS assay, our study demonstrated that compared to immortalized melanocytes (Mel-ST cells) all tested human melanoma cell lines exhibited a marked elevation of total NOS activities, although no correlations were evident with the metastasis status of tested cell lines (Fig. 1D).

### *nNOS expression is sensitive to UV radiation and growth factors and is elevated in melanoma compared to normal melanocytes*

As shown in Figure 2A, immunoblotting assay revealed that the nNOS expression levels in human melanoma cell lines were much higher compared to levels in primary normal human melanocytes. Since UVB-melanoma in the hepatocyte growth factor/scatter factor (HGF/SF) transgenic mouse melanoma model is well characterized and recapitulates fairly well the etiology and induced histopathology of human

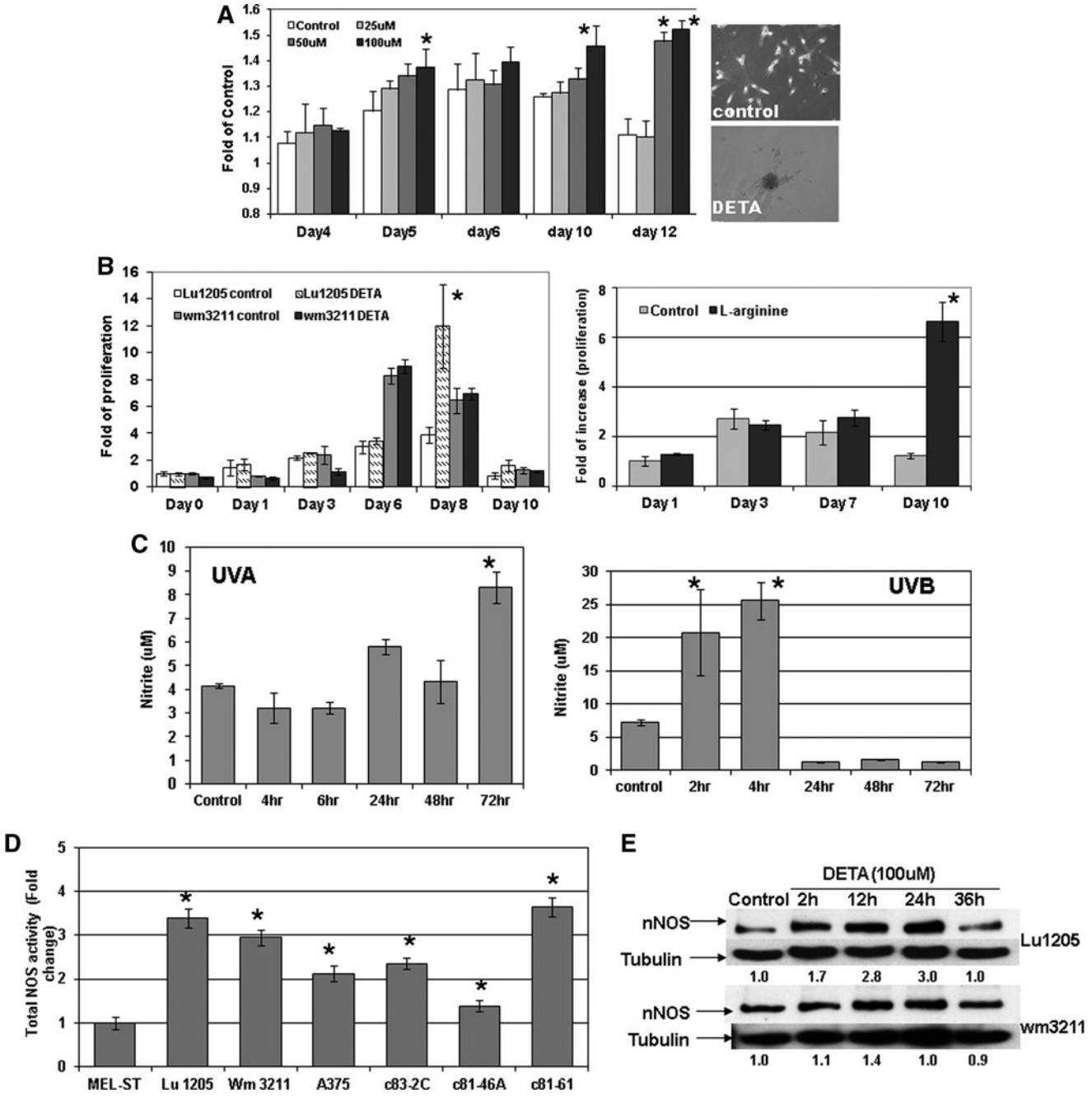


**FIG. 1. (A) Long-term treatment of (*Z*)-1-[2-(2-aminoethyl)-*N*-(2-ammonioethyl) amino] diazen-1-ium-1,2-diolate (DETA/NO) stimulates melanocyte proliferation and forms foci in cell culture.** The photos represent foci formed after 10 weeks. *$p < 0.05$ compared to control. **(B)** Nitric oxide (NO) stress generated by DETA/NO (100 $\mu M$) or L-arginine (2.87 m$M$) enhanced melanoma proliferation, more evident in metastatic cells. *$p < 0.05$ compared to control. **(C)** Both ultraviolet (UV) A (3 J/cm$^2$) and UVB (25 mJ/cm$^2$) radiation increased NO levels in primary melanoma wm3211 cells. Results represent the means ± SDs of three replicates. *$p < 0.05$ compared to control. **(D)** Increased total nitric oxide synthase (NOS) activities in melanoma cell lines compared to immortalized MEL-ST melanocytes. Results are expressed in folds of change standardized by Mel-ST cells for three biologic replicates. *$p < 0.05$ compared to Mel-ST cells. **(E)** Effects of DETA/NO treatment on nNOS expression levels in human melanoma cells. Whole cell lysates were collected after incubation with DETA/NO at different time points, followed by immunoblotting analysis. The relative expression levels of nNOS were normalized by tubulin levels. The presented values were standardized with control.

melanoma (43), we also carried out similar experiments with mouse cells that have been established from the developed lesions and used as the screening panel for translational or mechanistic studies. Similarly, immunoblotting study also showed markedly elevated nNOS expression compared to normal mouse melanocytes, especially in F5061 cells, which are aggressively tumorigenic and metastatic (Fig. 2B).

Consistent with what we have found *in vitro*, histologic examination and immunohistochemistry (IHC) staining revealed that nNOS levels detected in biopsies of melanoma

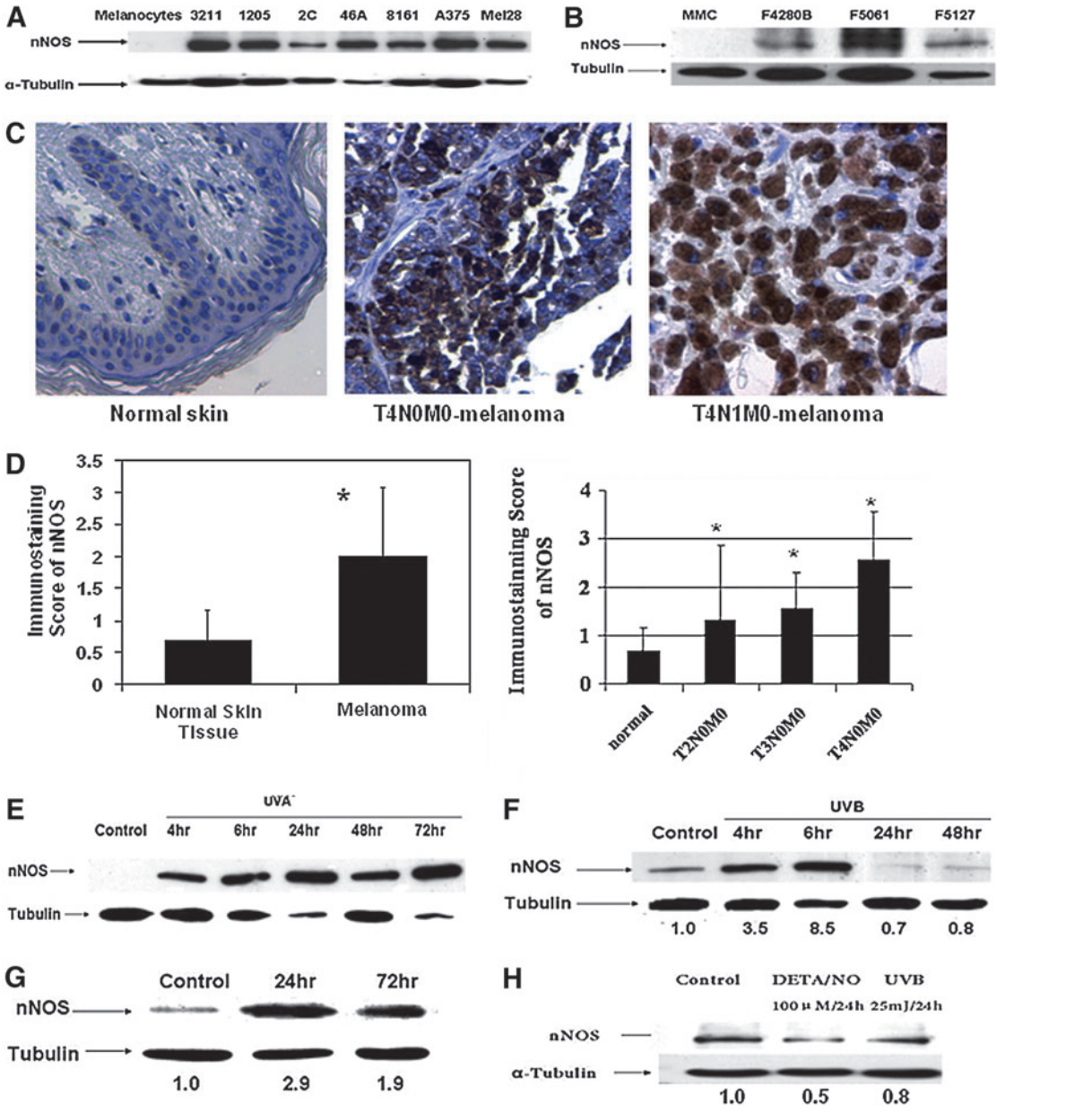


**FIG. 2. Neuronal NOS (nNOS) expression is elevated in melanoma compared to normal melanocytes. (A)** Immunoblotting assay of human primary melanocytes and melanoma cell lines. **(B)** Immunoblotting assay of mouse melanoma cell lines (F4280B, F5061, and F5127) and mouse melanocytes (MMC). **(C)** Immunohistochemistry analysis of nNOS expression levels using melanoma tissue array. Positive cells were visualized by light microscope and at least 10 highlight fields of each sample were examined. **(D)** Increased nNOS stainings in melanoma biopsies were significantly correlated with disease stages. Immunohistochemistry (IHC) staining score was determined by the average percentage of cells positive for nNOS: 0, 0%–5%; 1, 6%–30%; 2, 31%–59%; and 3, >60%. The number of samples in normal, T2N0M0, T3N0M0, and T4N0M0 were 23, 3, 9, and 10, respectively. *$p < 0.05$ compared to normal skin tissue. **(E, F)** nNOS expression is markedly induced by UVA **(E)** or UVB **(F)** radiation in human melanoma cells. The represented data were done in wm3211 cells. **(G, H)** Basic fibroblast growth factor (10 ng/ml) treatment stimulated nNOS expression in immortalized human melanocytes, but DETA/NO incubation and UVB radiation failed to induce nNOS levels in normal Caucasian melanocytes. To see this illustration in color, the reader is referred to the web version of this article at www.liebertpub.com/ars

were much higher than that of adjacent normal skin (Fig. 2C), and the average staining score of pooled melanoma samples was increased by 1.9-fold (Fig. 2D; $p < 0.05$). When grouping melanoma samples based on disease stage, we observed a trend of increased nNOS staining scores with melanoma progression from patient biopsies (trend analysis, $p < 0.0001$; Fig. 2D). The average score of T4N0M0 samples was 2.56, approximately twofold as compared to that of T2N0M0 samples, which are much thinner and at earlier stages (1.33).

Given that UV radiation induced a marked increase in NO levels, we investigated the effects of UV irradiation on nNOS expression. Notably, both UVA and UVB treatments

efficiently induced the expression of nNOS protein, but in different time-related patterns (Fig. 2E, F). The induction of nNOS by UVA lasted much longer (for at least 3 days), while UVB-induced nNOS peaked at 6 h and diminished quickly. Such distinct patterns coincided with NO level changes after UVA or UVB irradiation, indicating the direct involvement of nNOS in UV-induced NO production in melanoma cells.

Interestingly, in human immortalized melanocytes, the growth factor basic fibroblast growth factor (bFGF), which stimulates melanoma growth (5), markedly induced nNOS expression markedly (Fig. 2G). However, nNOS induction by UVB and DETA/NO, evident in melanoma cells, was not observed in primary melanocytes (Fig. 2H).

### *nNOS silencing was associated with reduced tumor growth and invasion potential in metastatic melanoma cells both* in vitro *and* in vivo

Using small interfering RNA (siRNA) transfection, we transiently knocked down nNOS in two metastatic melanoma cells (A375 and Lu1205) (Fig. 3A). Immunoblotting analysis showed that with nNOS depletion, the expression levels of JunD, MMP-1, APE/Ref-1, and Bcl-2 were significantly reduced, which are well-known genes that contribute to melanoma proliferation and invasion (58,59,61).

Utilizing lentiviral-based shRNA, we successfully established melanoma cell lines (A375 and Lu1205) with stable nNOS knockdown for further *in vivo* lost-of-function studies (Fig. 3B). In parallel with decreased MMP-1 expression, the invasion potential of metastatic melanoma was markedly decreased by stable nNOS depletion as assessed by matrigel invasion assay (Fig. 3C and Supplementary Fig. S2).

To investigate whether nNOS depletion affects melanoma growth and metastases *in vivo*, we inoculated human metastatic melanoma A375 cells carrying control shRNA or nNOS shRNA, respectively, into nude mice. In contrast with the highly aggressive tumor growth of A375/control cells, inoculation of nNOS-depleted cells exhibited a predominant reduction of the size of tumor xenografts, thereby suggesting the antimelanoma capacity with loss of nNOS function (Fig. 3D). By the end of the experiment, as shown in Figure 3E and F, the average weight of xenografted tumors was significantly decreased to 53% of control group (control: 1.13 g; nNOS shRNA: 0.60 g; $p < 0.001$). No statistic difference in body weight occurred between the two experimental groups. Similar inhibitions of tumor growth by nNOS knockdown were also evident in Lu1205 cells (Supp Fig. S3).

At the end of the experiment, the lung tissue of each mouse was also carefully removed and weighed. The metastases identified in the lung were determined by positive HMB-45 immunohistochemical staining, which is a typical biomarker of human melanoma cells (Fig. 3H). Histological sections of control lungs showed considerable strong positive staining in four out of five mice (80%); however, the lung metastases with positive HMB-45 staining were only developed in two of five mice inoculated with nNOS-depleted melanoma cells (40%). The HMB-45 staining densities were also lighter compared to control samples (Fig. 3H). Consistently, the lung wet weight of the nNOS knockdown group was reduced significantly compared to that of control samples as shown in Figure 3G ($p < 0.05$, $N = 5$).

### *Effects of nNOS inhibitor cpd8 on human melanoma cells*

We tested a number of synthesized nNOS inhibitors as listed in Table 1. The candidate compounds with lower $K_i$/nNOS values exhibited higher binding affinities and more potent enzyme inhibition. The calculated values of $K_i$(eNOS)/$K_i$(nNOS) and $K_i$(iNOS)/$K_i$(nNOS) represented the relative selectivity of nNOS over eNOS or iNOS, respectively. Among these compounds, cpd8 (Fig. 4A) exhibits 3000-fold selectivity for nNOS over eNOS and 840-fold selectivity over iNOS. Further, cpd8 binds tightly to nNOS and its $K_i$(nNOS) is very low (17.7 n*M*).

At 1 $\mu M$ concentration, cpd8 effectively inhibited the NOS activity in metastatic Lu1205 cells; however, its inhibitory activity decreased after 48 h, suggesting that the inhibition of nNOS by cpd8 is potent but reversible (Fig. 4B). Spermidine trihydrochloride, a commercially available nNOS inhibitor, generated a comparable inhibition of NOS activity at a concentration of 10 $\mu M$; 10-fold of cpd8.

Although cpd8 does not affect basal nNOS levels of melanoma cells up to a concentration of 200 $\mu M$ (not shown), cpd8, as low as 1 $\mu M$ concentration, effectively inhibited the induction of nNOS by DETA/NO or UVB radiation treatments (Fig. 4C, D). As shown in Figure 4E, DETA/NO-stimulated proliferation was significantly reversed by cpd8 cotreatment. Similar reduction in cell invasion potential was also evident by cpd8 cotreatment, which efficiently alleviated the increased invasion by DETA/NO exposure (Fig. 4F). Notably, as shown in Supplementary Fig. S7, cpd8 exhibited no apparent cytotoxic effect on human primary fibroblast cells, keratinocytes, and immortalized melanocytes up to 100 uM.

### *L-Arginine significantly enhanced the growth and invasion of human melanoma due to nNOS-mediated NO stress, which is effectively inhibited by nNOS inhibitors but not iNOS inhibitors*

As shown in Figure 5A, an *in vitro* matrigel-coated chamber invasion assay demonstrated that incubating metastatic melanoma cells with L-arginine (2.87 m*M*), a NOS substrate, markedly enhanced the invasion potential, which was efficiently reversed by cotreatment with nNOS inhibitor cpd8. Immunoblotting analysis revealed the induction of nNOS protein expression by L-arginine incubation, which peaked quickly after exposure for 4 h (Fig. 5B). Our *in vitro* study also showed that L-arginine treatment significantly stimulated cell proliferation in melanoma Sk-Mel28 cells (Fig. 1B and Supp Fig. S12). In addition, we constructed artificial human skin equivalents in a three-dimensional (3D) setting incorporating human metastatic melanoma cells, keratinocytes, and fibroblast cells on a collagen base. As shown in Figure 5C, after 2 weeks of treatment, L-arginine significantly promoted melanoma growth compared to control and melanoma lesions spread over the epidermis layer. Some of these lesions grew deeper and invaded downward toward the dermal layer. All the lesions were stained positively for melanocyte marker S100 (Supplementary Fig. S6). Cotreatment with nNOS inhibitor cpd8 (2 $\mu M$) reversed the overgrowth induced by L-arginine, and the skin reconstruct samples looked much like the control with a smooth epidermal surface.

To investigate whether L-arginine-induced NO generation in melanoma is mediated by nNOS, we incubated nNOS-

depleted cells with L-arginine and analyzed intracellular NO levels. As shown in Figure 5D, L-arginine failed to induce NO production in nNOS-depleted cells, which indicated that L-arginine-induced NO generation in melanoma was predominantly mediated by nNOS utilizing L-arginine as the substrate. Notably, the induction of NO levels that occurred after L-arginine exposure was only reduced by the nNOS inhibitor cpd8 (Fig. 5E). Increased amounts of resveratrol and curcumin (up to 50 $\mu M$, two well-documented iNOS inhibitors) failed to inhibit the increase of NO by L-arginine in human melanoma cells. Consistently, as shown in Figure 5F, other commercially available iNOS inhibitors such as 1400W and aminoguanidine (1 $\mu M$) exhibited no significant inhibition on melanoma invasion after 24 h of treatment. In addition, the adhesion of melanoma cells to fibroblasts was only marginally reduced by exposure to 10 $\mu M$ 1400W treatments ($p > 0.05$), while, notably, cpd8 at 1 $\mu M$ markedly inhibited melanoma adhesion potential compared to control (Fig. 5G).

### *Novel nNOS inhibitors showed promising antimelanoma activities*

As shown in Figure 6A, all tested nNOS inhibitors efficiently diminished UVA-induced NO production at 1 $\mu M$ concentration. With a cotreatment, NO levels, in most of the samples, were reduced to basal levels comparable to that of control. Treatments with these inhibitors alone also significantly reduced the invasion potential of metastatic melanoma A375 cells (Fig. 6B). Further, cell adhesion analysis revealed that short-term treatments with nNOS inhibitors significantly inhibited L-arginine-stimulated adhesion of metastatic A375 cells to human primary fibroblast cells (Fig. 6C). At a concentration of 2 $\mu M$, cpd8 exhibited the most potent inhibitory effect among all the tested inhibitors of relative adhesion compared to L-arginine alone.

To determine whether the inhibitions of nNOS correlated with their anti-invasive activities, we employed linear regression analysis utilizing SAS statistic software (Supplementary Fig. S11). Our correlation analysis of anti-invasion potential and iNOS inhibitory potency [represented as $1/K_i$(iNOS)] has produced an $R^2$ of 0.0153 ($p = 0.7917$) and for nNOS inhibition potency [represented as $1/K_i$(nNOS)], an $R^2$ value of 0.1467 ($p = 0.3964$) was obtained. No significant correlation was detected by our analysis ($p > 0.05$).

Notably, cpd2 (Table 1) showed promising cytotoxicities in our tested melanoma cell lines (wm3211 and Sk-Mel28), and the $IC_{50}$ was 5 and 3.5 $\mu M$, respectively (Fig. 6D); however, on the contrary, up to 5 $\mu M$ cpd2 exhibited no predominant effects on cell viability in human immortalized melanocytes (Supp Fig. S4). Such selectivity will definitely be advantageous for *in vivo* treatment with reduced side toxicities. In addition, further structure–activity analysis demonstrated that the antimelanoma potency may be related to the phenyl group attached to the pyrrolidine N atom, and since the homolog of cpd2, which is the same as cpd2 except that the phenyl group is absent, does not exhibit any toxicity to melanoma cells, even up to 50 $\mu M$ (Supp Fig. S1).

In contrast to cpd2, the commercially available iNOS inhibitor 1400W (100 $\mu M$) exhibited no apparent inhibitory effects on melanoma cell proliferation (as shown in Supplementary Fig. S5).

## Discussion

In the United States, there is a rapidly increasing incidence of CM, which is becoming a substantial public health concern (50). In this study, we identified the potential connections between nNOS/NO stress and melanoma progression. We have shown that in melanoma, nNOS, which is sensitive to UV radiation, is associated with the increased generation of intracellular NO, which in-turn stimulates proliferation and invasion. Utilizing novel highly selective nNOS inhibitors significantly reduced the invasion potential of melanoma cells *in vitro*. Consistently, our study has also demonstrated the significant growth inhibition and suppression of pulmonary metastasis by stable nNOS depletion in highly metastasizing melanoma cells *in vivo*. It may thus be possible to target nNOS with specific inhibitors as an effective novel strategy for the prevention and treatment of melanoma.

### *Why is nNOS important for melanoma development?*

iNOS is markedly induced after UV radiation such as a sunburn, and plays an important role in carcinogenesis and skin tumor development which has been well documented in many human and animal studies (8,15,24). In human melanoma, studies also demonstrated that iNOS expression was associated with poor survival and predicted metastasis (13,16,56). Specific iNOS inhibitors were shown to inhibit melanoma growth (42,51); however, when looking into the specific iNOS inhibitors tested in these studies we noticed that these compounds actually were not so selective for iNOS inhibition (7,32). For example, the $K_i$ value for iNOS and nNOS of compound 1,4-PBIT was 7.4 and 16 n$M$, respectively, indicating that the iNOS selectivity over nNOS was only 2.2-fold. We concluded that the reduction

**FIG. 3. Effects of nNOS depletion on melanoma invasion and growth. (A, B)** nNOS depletion in melanoma is associated with downregulation of genes involved in proliferation and invasion. Metastatic melanoma cells were transfected with either nNOS small interfering RNA (siRNA) (**A**, Lu1205 cells) or lentiviral shRNA-nNOS (**B**, A375 cells). Whole cell lysates were collected for immunoblotting assay. **(C)** Matrigel invasion assay. The represented data were from A375 metastatic melanoma cells with stable nNOS knockdown. Similar changes were also evident in Lu1205 cells (Supplementary Fig. S2). **(D–G)** Stable knockdown of nNOS inhibited tumor growth and prevented lung metastases *in vivo* in a xenograft mouse model. About $1 \times 10^6$ A375/control-shRNA or A375/nNOS-shRNA cells were injected to nude mouse subcutaneously on blank. The growth of tumor **(D)** was measured three times a week. Tumor volume was calculated as: tumor volume ($mm^3$) = (length/2) × (width)$^2$. The weight of final harvested tumor xenografts (g, *panel* **F**) and relative lung wet weight (mg/g body weight, *panel* **G**) were measured by the end of experiment. $^*p < 0.05$ compared to control ones that were injected with A375 cells carrying shRNA-control construct. $N = 10$. *Bars*: mean ± SD. $^*p < 0.05$. **(H)** Successive sections from paraffin-embedded lung tissues were immunohistochemically stained with antibody against HMB-45 to confirm the lung metastases of melanoma xenograft tumor model. Nuclei were counterstained with hematoxylin. To see this illustration in color, the reader is referred to the web version of this article at www.liebertpub.com/ars

of melanoma growth caused by these compounds cannot be due solely to iNOS blocking. In addition, poor cellular permeability of these compounds and their associated systemic toxicity have limited their potential success in the clinic.

Many candidate chemopreventive agents such as natural products found in fruits and herbs (resveratrol and curcumin), exhibit potent inhibitory effects on NO generation and, specifically, modulation of iNOS expression; chemoprevention activity has been observed in a wide range of *in vitro* and *in vivo* studies (30,53). However, in melanoma cells, increased intracellular NO generation by L-arginine supplementation was not affected at all in our studies by resveratrol and curcumin even up to a concentration of 50 $\mu M$. On the other hand, the nNOS inhibitor cpd8, at as low a concentration of 1 $\mu M$,

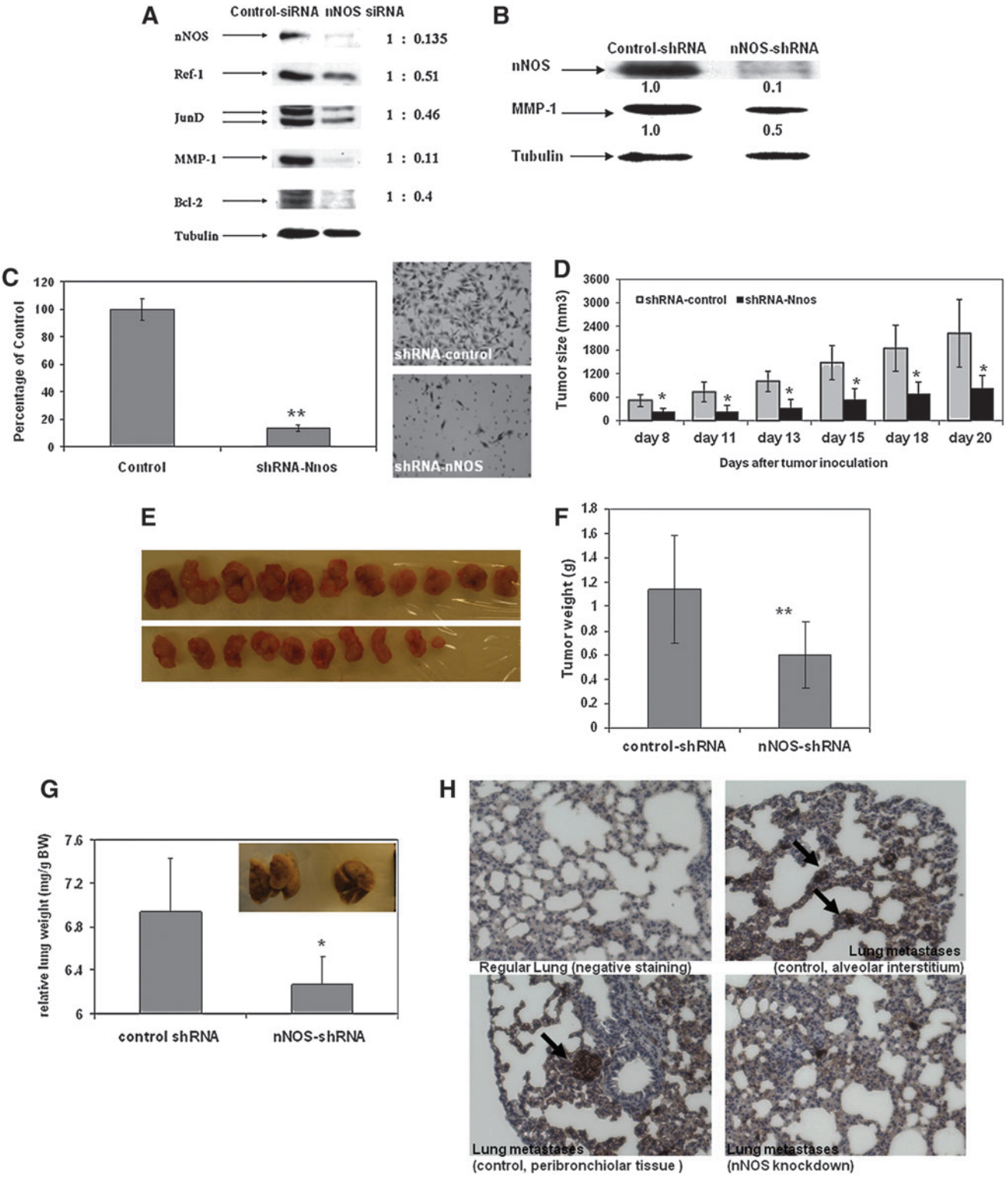

Table 1. Novel Synthesized Neuronal Nitric Oxide Synthase Inhibitors with Various Selectivity and Potency on Neuronal Nitric Oxide Synthase Activity

| | $K_i$ (μM) | | | Selectivity | |
|---|---|---|---|---|---|
| *Compounds (cpd)* | *nNOS* | *iNOS* | *eNOS* | *nNOS/iNOS* | *nNOS/eNOS* |
| 1 | 0.014 | 4.06 | 28 | 290 | 2000 |
| 2 | 48 | 609 | 122 | 12.7 | 2.5 |
| 3 | 0.21 | 13.6 | 116 | 64.8 | 552.4 |
| 4 | 0.088 | 18.2 | 123.9 | 207 | 1408 |
| 5 | 0.098 | 5.84 | 282.9 | 59.6 | 2886.7 |
| 6 | 0.085 | 8.95 | 85.16 | 105.3 | 1001.9 |
| 7 | 0.024 | 5.4 | 78.45 | 225 | 3268.8 |
| 8 | 0.0177 | 15 | 53.4 | 847.4 | 3017 |

nNOS/iNOS represents the selectivity of nNOS over iNOS, calculated by $K_i$(iNOS)/$K_i$(nNOS); nNOS/eNOS represents the selectivity of nNOS over eNOS, calculated by $K_i$(eNOS)/$K_i$(nNOS).
nNOS, neuronal nitric oxide synthase; iNOS, inducible NOS; eNOS, endothelial NOS.

efficiently inhibited NO production in melanoma, indicating that the NO generation is predominantly mediated by nNOS rather than iNOS.

A prior study showed that iNOS was expressed *de novo* in most benign pigment cell lesions, while iNOS played a less significant role in vertical growth phase and in metastatic melanoma (3). In our histological study of melanoma biopsies, there was a significant trend of nNOS staining increasing with disease stage suggesting that nNOS staining may serve as an adjunct biomarker for melanoma diagnosis. We propose that NO stress mediated by nNOS contributes more to disease progression rather than serving as an initiating event, which has also been supported by our *in vivo* studies. We did not observe a significant delay of tumor occurrence after inoculation, but the tumor growth rate and lung metastases were prominently inhibited by nNOS depletion.

In addition, even at a much higher concentration, compared to nNOS inhibitor cpd8 commercially available iNOS inhibitors failed to effectively inhibit melanoma proliferation and invasion, which strongly supported our argument that targeting nNOS signaling is not only a novel but could potentially be an effective intervention for human melanoma.

### *Distinct effects of UVA and UVB radiation on nNOS activity and expression patterns*

There is much disagreement regarding the relative roles of UVA and UVB in melanomagenesis. In many transgenic mouse and *Xiphophorus* hybrid fish models, UVB, but not UVA, exhibits carcinogenesis potential and induced melanoma lesions (10,41). However, recent epidemiological studies suggest an involvement of UVA in the genesis of CM as well (4). Interestingly, our study exhibited distinct effects of UVA and UVB on nNOS induction and NO generation, suggesting that their regulatory mechanisms are different.

The large increases of nNOS expression induced by UVA lasted for at least 72 h with significantly elevated intracellular NO production. However, one study showed that in human keratinocytes, UVA-mediated NO formation was nonenzymatic and came from "NO storage" in the skin (29). Therefore, the induction of nNOS/NO by UVA might be of specific importance for melanoma cells. UVB-induced nNOS occurred in a transient, short-duration manner; the induction of NO was evident shortly after UVB exposure and peaked at 4 h followed by a sharp drop. Although similar transient nNOS induction after UVB exposure was reported in HaCaT kerationcytes, the predominant elevation of NO levels was mediated by iNOS induction especially in the late phase post-UVB (>6 h) (31). We propose that the long-lasting nNOS induction by UVA might account for delayed chronic responses; the transient nNOS induction by UVB might contribute to acute reactions. Determination of the detailed regulation mechanisms will need to be characterized and defined in future studies. In addition, we failed to detect any significant changes of iNOS or eNOS expression levels in wm3211 cells after UVA radiation (Supplementary Fig. S8), which, from another point of view, further demonstrated the predominant role of nNOS in UV-activated NO signaling in human melanoma.

### *L-Arginine, the substrate of nNOS, enhances the growth and invasion of melanoma*

In human melanoma, L-arginine is of particular importance. One reason is that, in melanoma cells, L-arginine serves as the substrate for overexpressed nNOS to generate NO; another reason lies in the special amino acid metabolism that occurs in melanoma. In normal tissues, arginine is not an essential amino acid, but melanoma depends on an exogenous supply of arginine due to the lack of *de novo* argininosuccinate synthetase (49). Currently, recombinant arginine deiminase, an Arg-degrading enzyme, is in Phase II clinical trials for metastatic melanoma patients (60). Our study showed that L-arginine significantly enhanced the invasion potential of melanoma cells with increased NO production and stimulated melanoma overgrowth in a 3D skin reconstruct. Notably, in addition to serving as an enzyme substrate, our study also showed that L-arginine incubation induced nNOS expression levels which further enhanced intracellular NO generation. The mechanism underlying such induction by L-arginine might be due to an NO-mediated feed forward activation of NOS as we have reported previously (61), but details need to be outlined in future studies. Consistently, in melanoma, the knockdown of nNOS or the utilization of specific nNOS inhibitors reversed the effects of L-arginine suggesting that the stimulating effects of L-arginine, at least in part, resulted from nNOS-mediated NO stress. The combination of L-arginine deprivation (*via* diet manipulation) with nNOS inhibition might achieve a better antimelanoma efficacy.

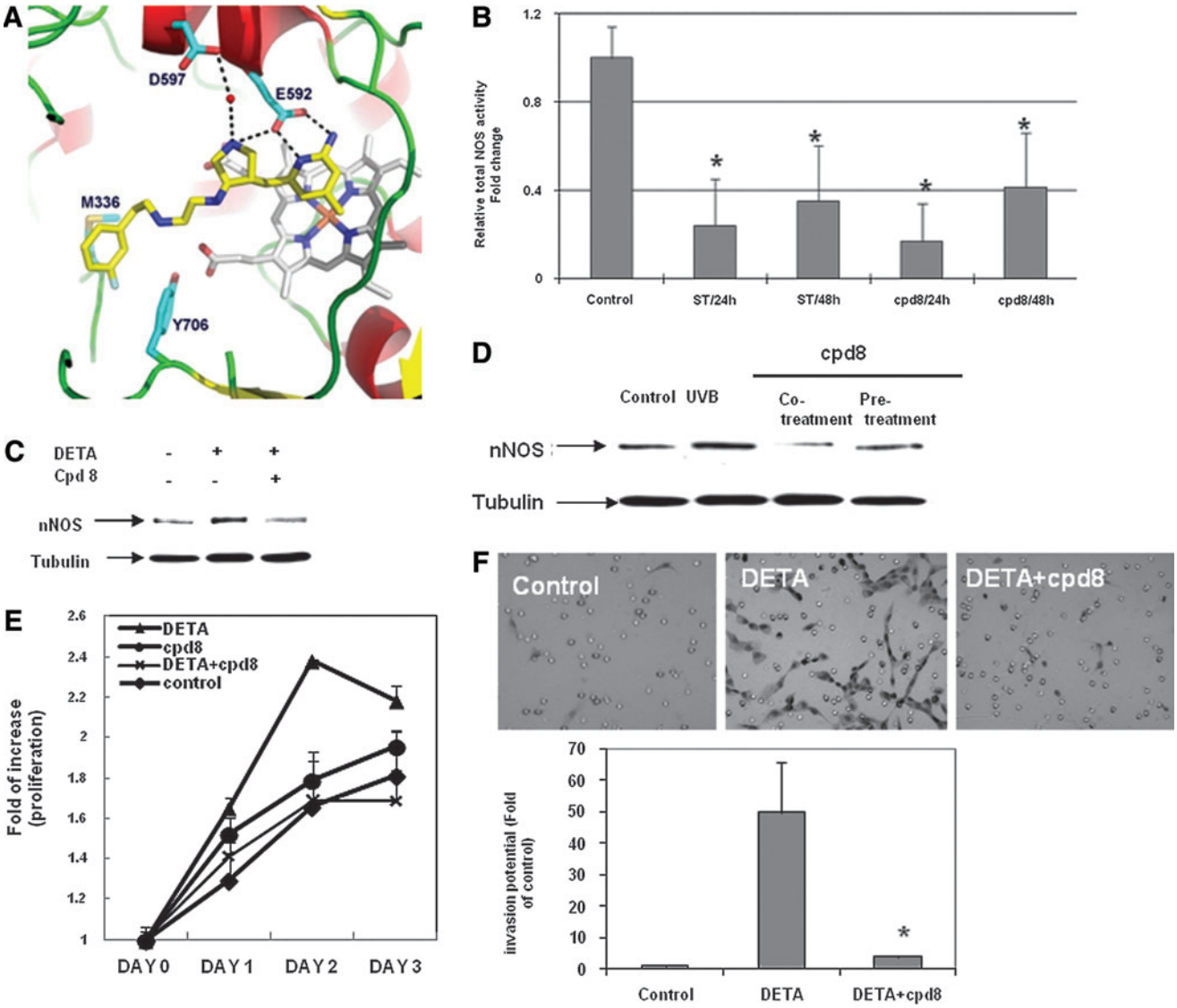


**FIG. 4. Specific nNOS inhibitor cpd8. (A)** Docking model of cpd8 with nNOS protein. **(B)** cpd8 significantly reduced total NOS activities in human melanoma Lu1205 cells. Spermidine trihydrochloride (ST), 10 $\mu M$; cpd8, 1 $\mu M$. Results are the mean ± SD of three biologic replicates of a representative experiment. *$p < 0.05$ compared to control cells. **(C, D)** cpd8 inhibited nNOS expression induced by DETA/NO stress **(C)** and UVB radiation **(D)**. Pretreatment: pretreated with cpd8 for 24 h, followed by UVB radiation; cotreatment: radiated by UVB, then replaced with fresh growth media containing cpd8. Twenty-four hours later, whole cell lysates were collected for immunoblotting analysis. **(E, F)** Elevated proliferation **(E)** and invasion potential **(F)** by DETA/NO stress were also reversed by cpd8 cotreatment. *$p < 0.05$, compared to DETA alone ($n = 2$). Proliferation was detected by MTT colorimetric assay ($n = 3$). To see this illustration in color, the reader is referred to the web version of this article at www.liebertpub.com/ars

### *Inhibition of nNOS with novel inhibitors*

NOSs consist of a reductase domain, an oxygenase domain, and the substrate L-arginine. Although the three mammalian NOS isoforms (iNOS, nNOS, and eNOS) share ~50% amino acid identity (26), the crystal structures of the oxygenase domains (where substrate oxidation occurs) showed that the active sites are nearly identical (9). As a result, isoform-selective drug design is a challenging problem with NOS. Most early efforts were directed at making nonselective NOS substrate analog inhibitors, which, however, could be harmful by interfering with other essential functions of NO. Although one study showed that the nonselective NOS inhibitor N[G]-amino-L-arginine sensitized ovarian cancer cells to cisplatin with enhanced apoptosis (27), its low potency precluded potential clinical benefit. Therefore, to minimize side effects, high selectivity is very critical in the design of NOS inhibitors.

Nevertheless, the Poulos and Silverman labs have successfully elucidated the structural basis for a group of highly selective nNOS inhibitors and designed new classes of more potent drug-like inhibitors (22,23,52). In our studies, we have tested a group of these potent nNOS inhibitors with distinct $K_i$ values for nNOS, iNOS, and eNOS, which efficiently inhibited UVA-induced NO production and reduced the invasion potential of metastatic melanoma cells. We correlated their iNOS or nNOS inhibitory potency with observed anti-invasion

activities, but due to the limited number of samples available no significant correlations were identified (Supplementary Fig. S11); however, a positive regression curve was more evident for nNOS, suggesting that the inhibitory effects of nNOS are more related to melanoma inhibition as compared to that of iNOS or eNOS. With more compounds synthesized and examined, we hope to achieve enough statistic power to confirm such a trend of correlation in our future studies.

Notably, among our screened nNOS inhibitors, cpd2, which shows a relatively weak nNOS selectivity and inhibition potency, has exhibited promising cytotoxicities in human melanoma. At concentration $\leq 5\,\mu M$, cpd2 exhibited no apparent toxicities in human immortalized melanocytes. In our future studies, we will perform more extensive structure/activity comparisons to identify the key modalities that enhance nNOS inhibition potential and improve the selective antimelanoma activities before embarking on *in vivo* mouse studies.

## Materials and Methods

### *Cell culture*

Human melanocytes were isolated from new-born foreskin following the procedure described previously (57), and cultured in MCDB153 medium (Sigma, St. Louis, MO). Primary fibroblast cells and keratinocytes were also isolated from foreskins (20), and cultured in Dulbecco's Modified Eagle Medium (DMEM) and EpiLife medium, respectively (<10 passages). Primary melanoma wm3211 and metastatic melanoma A375, Lu1205, Sk-Mel-28, c83-2c, c81-61, and c81-46A cells were cultured as described previously (57). Human immortalized melanocyte cell line Mel-ST was generously gifted by Dr. Weinberg and cultured in DMEM supplied with fetal bovine serum (FBS).

Mouse melanocytes (Melan-A) were cultured in RPMI1640 medium supplied with 10% FBS, pennicillin/streptomycin, 0.1 m*M* 2-mercaptoethanol, and 200 n*M* 12-O-Tetradecanoylphorbol 13-acetate. Mouse melanoma cells F5061, F4280b, and F5127 were established in melanoma lesions developed in HGF/SF transgenic mouse and were cultured in DMEM.

### *Materials*

The NO donor DETA/NO (Alexis Biochemicals) was dissolved in phosphate buffered saline and used at a concentration of $100\,\mu M$. Resveratrol and curcumin were purchased from Sigma Life Sciences, dissolved in dimethyl sulfoxide, and used at a concentration of $50\,\mu M$. L-arginine was also ordered from Sigma and the final concentration used in our study is 2.87 m*M*. Antibodies used for immunoblotting analysis [JunD, MMP-1, Bcl-2, S-100, and nNOS (SC-17825)] were from Santa Cruz Biotechnology; α-tubulin or β-actin antibody was from Sigma Life Sciences; and APE/Ref-1 antibody was from Novus Biologicals.

### *Tissue array and IHC staining*

A human melanoma tissue array (ME482) was purchased from U.S. Biomax, Inc. The tissue array includes matched normal skin tissues that were biopsied from the adjacent tissue of each cancer tissue from individual patients. The HRP-AEC Chromogen staining kit (R&D Systems) was used to visualize the expression levels of nNOS. Briefly, the slide was deparaffinized and rehydrated through a graded series of ethanol. After sequential blockings with peroxidase/serum/avidin/biotin blocking reagents, the slide was incubated with nNOS antibody (1:500) at 4°C overnight. Following washes, the secondary biotinylated anti-mouse antibody (1:200) and HSS-HRP were sequentially applied for 30 min at room temperature, and the reaction product was visualized with hydrogen peroxide and AEC as chromogenic substrate, which revealed a bright red immunoreactivity. For S-100 and HMB-45 staining, slides were incubated with S-100 and HMB-45 antibodies, respectively, and the staining was visualized by DAB kit (Santa Cruz Biotech), which develops a brown color. All the samples were counterstained by hematoxylin.

### *Cell protein extraction and Western blot analysis*

Melanoma cells were collected and lysed as described previously (61). Equal amounts of protein samples were subjected to sodium dodecyl sulfate polyacrylamide gel electrophoresis, and transferred to nitrocellulose membranes. The specific protein was then detected by the antibodies [anti-APE/Ref-1 (1:3500), anti-nNOS, anti-Bcl-2 and anti-MMP-1 (1:1000), anti-AP-1/JunD and anti-α-tubulin or anti-actin (1:1000)] followed by a chemiluminescence detection reagent (Peirce). Signal intensity on membranes was measured using an imaging densitometer with Multi-Analyst software (Bio-Rad). All data were expressed as fold change of the control based on the calculation of density values of the specific protein bands standardized by α-tubulin/actin.

**FIG. 5. L-Arginine enhanced the invasion and growth of human melanoma, which is mediated by nNOS/NO signal pathway and was effectively inhibited by nNOS inhibitor. (A)** Matrigel invasion analysis of melanoma A375 cells. Elevated invasion potential by L-arginine was inhibited by cpd8 cotreatment. $^{\#}p<0.05$ compared to control; $^{*}p<0.05$ compared to L-arginine alone ($n=3$). **(B)** Effects of L-arginine on nNOS expression levels in melanoma A375 cells. Whole cell lysates were collected after incubation with L-arginine at different time points (final concentration: 2.87 m*M*), followed by immunoblotting analysis. The relative expression level of nNOS was also normalized by the tubulin levels. **(C)** Histology of melanoma growth stimulated by L-arginine in reconstructed skin equivalents, which were incubated in the absence or presence of cpd8. The represented samples were stained with hematoxylin and eosin. **(D)** Intracellular NO level was increased by 4 h after incubation with L-arginine, which was markedly diminished by nNOS depletion in A375 cells. $^{\#}p<0.05$, compared to control; $^{*}p<0.05$, compared to control siRNA/L-arginine ($n=3$). **(E)** L-Arginine-induced NO generation was only inhibited by nNOS inhibitor cpd8 after coincubation for 24 h. RES, resveratrol; CUR, curcumin, $50\,\mu M$; cpd8, $1\,\mu M$. $^{\#}p<0.05$, compared to control; $^{*}p<0.05$, compared to L-arginine alone ($n=3$). **(F, G)** No effects of iNOS inhibitors (1400W and aminoguanidine) on melanoma invasion **(E)** and adhesion **(F)** were observed. Same amount of melanoma Sk-Mel28 cells were seeded in the upper part of matrigel-coated transwells with presence of different compounds at $1\,\mu M$ for 24 h before harvested for matrigel invasion analysis. For adhesion analysis, melanoma cells were seeded on top of fibroblast cell monolayer and incubated with different compounds at $10\,\mu M$ for 1 h, followed by MTT colorimetric assay. $^{\#}p>0.05$; $^{*}p<0.05$ compared to control. To see this illustration in color, the reader is referred to the web version of this article at www.liebertpub.com/ars

*Measurements of intracellular NO levels and NOS activities*

NO was measured as nitrite by interaction with Griess reagent (Enzo Life Sciences). Briefly, after treatments, $1\times10^6$ cells were collected and cell lysis buffer was added to each sample. Freshly collected whole cell lysates were then reacted with Griess reagent for detecting nitrite concentrations according to nitrite standard curve. The NOS enzyme activity was analyzed by ultrasensitive colorimetric assay according to the manufacturer's protocol (Oxford Biomedical Research, Inc.).

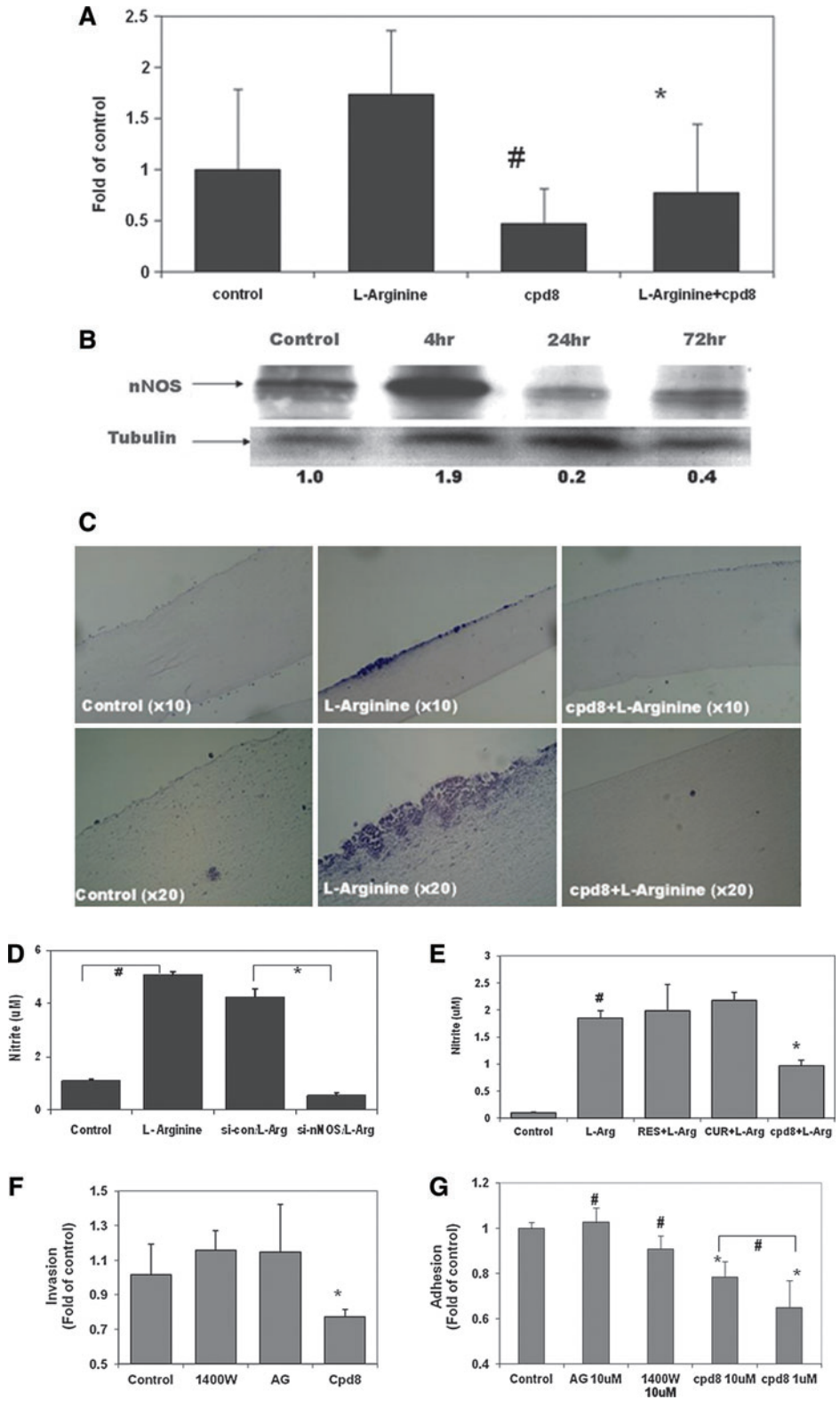

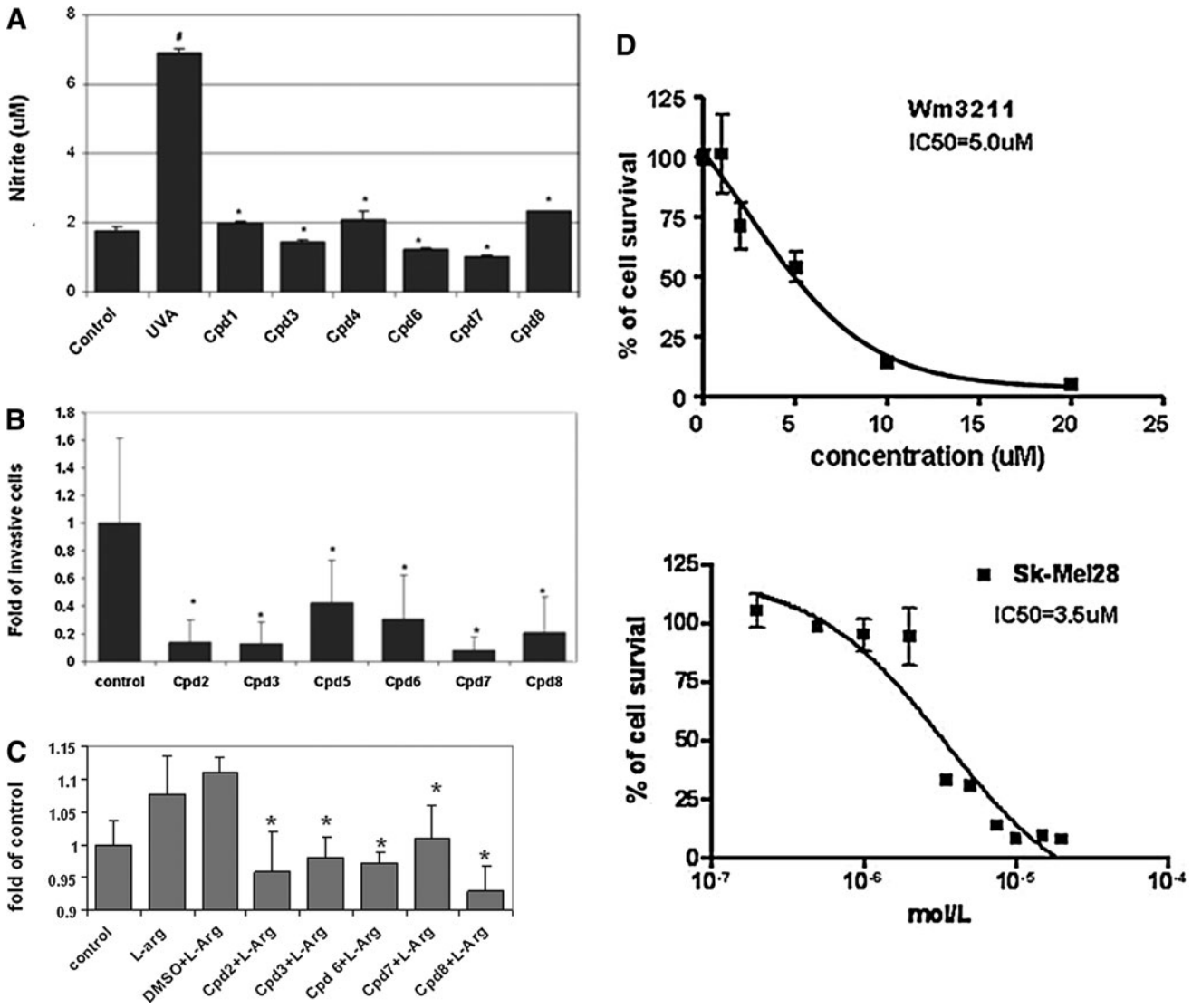


**FIG. 6. Effects of novel synthesized nNOS inhibitors on human melanoma cells. (A)** Inhibition of UVA radiation-induced intracellular NO generation detected by Griess reagents. $^{\#}p < 0.05$ compared to control; $^{*}p < 0.05$ compared to UVA-treated sample ($n = 3$); **(B)** Reduced invasion potential of metastatic melanoma. Bars represent the means of invaded cells counted in 20 highlight fields and normalized to control (set as 1.0). $^{*}p < 0.05$ compared to control ($n = 2$). **(C)** L-arginine-stimulated adhesion of metastatic melanoma A375 cells to fibroblast monolayer were inhibited by nNOS inhibitors. Cells were seeded on top of fibroblast monolayer in the presence of different nNOS inhibitors (2 $\mu M$) for 1 h. The data were represented as fold of control. $^{*}p < 0.05$ compared to DMSO + L-arginine treatment ($n = 3$). **(D)** Cytotoxicity of cpd2 in human melanoma cell lines by MTT assay ($n = 3$).

### *Matrigel invasion assay*

The invasiveness of melanoma cells were assessed based on the invasion of cells through matrigel-coated membrane (BD Biosciences). Briefly, melanoma cells were collected and reconstituted in a serum-free medium. Prepared cells were added to the upper matrigel-coated insert. After a 20 h incubation period, cells were fixed and stained with hematoxylin. Membranes were visualized microscopically and the invading cells on each of triplicate membranes were counted and averaged for 20 random fields.

### *Transient siRNA and stable shRNA transfection studies*

siRNA duplexes directed against *NOS1* (*nNOS*) were purchased directly from Sigma-Aldrich (NM_000620). About $1 \times 10^5$ cells were seeded in a six-well plate. After 24 h, the cells were transfected with nNOS siRNA or control siRNA (Mission® siRNA Universal Negative Control #1) to give the final concentration of 60 n*M* according to the manufacturer's directions *via* Lipofectamine (Invitrogen, Inc.). Thirty hours later, treat cells with L-arginine or collect whole cell lysates for immunoblotting analysis.

The GIPZ lentiviral shRNAmir (Open Biosystem) targeting human nNOS was utilized for stable loss-of-function studies including control shRNA. Replication-defective lentiviral virions were produced by transient cotransfection of pCMV and pMP2G vectors into HEK293T cells with Lipofectamine 2000 (Invitrogen). The media was changed 6 h after transfection and supernatant containing the virus was harvested 48 h after transfection, and filtered through 0.45-$\mu$m Stericup filters (Millipore). The virus was subsequently aliquoted and supernatants were stored at −80°C. Preseeded human

melanoma cells (A375 and Lu1205) were incubated with lentivirus-containing supernatant in the presence of hexadimethrine bromide (8 $\mu$g/ml) in flasks for 24 h. To establish cells with stable integrating shRNA constructs, replace media with fresh puromycin-containing media every 3 days until resistant colonies can be identified. Cells with stable expression of shRNA were confirmed by immunoblotting assay and collected for further *in vitro* and *in vivo* studies.

### *3D skin reconstructs*

Epidermal equivalents were constructed by mixing metastatic melanoma A375 cells with keratinocytes at a ratio of 1:15. Once the epidermis is adhered to the dermal layer, skin equivalents are then lifted to the air–liquid interface to allow keratinocyte differentiation. In terms of treatments, L-arginine (2.87 m*M*), with the presence or absence of nNOS inhibitor cpd8, was added directly to the culture medium from the lift-up day for 2 weeks. By the end of the experiments, the skin equivalents were fixed and stained with hematoxylin and eosin for pathological evaluation. S-100 staining as a melanocyte biomarker was performed to visualize and confirm the melanoma lesions (20).

### *Animals and melanoma xenograft* in vivo *model*

All the animal procedures were approved by the Institutional Animal Care and Use Committee at University of California Irvine. Male immunodeficient Balb/C nude mice purchased from Charles River were housed and maintained in UCI animal care facilities under specific pathogen-free conditions. Human melanoma cells were collected in single-cell suspension and the subcutaneous xenograft tumor model was generated by subcutaneously inoculating melanoma cells into nude mice ($1\times10^6$ cells in 100 $\mu$l volume per mouse). The growth of solid tumor xenografts was monitored three times a week and measured using vernier calipers. The size of subcutaneous tumors was calculated as tumor volume ($mm^3$) = $[L\times(W^2)]/2$. The mice were scarified at the end of experiment on day 21. The tumor xenografts and lungs were carefully removed, weighed, and fixed in formalin solution. To examine the macrometastatic nodules in lungs, immunohistochemical HMB-45 staining was applied subsequently to determine the presence of lung metastases of human melanoma cells.

### *Synthesis of novel nNOS inhibitors and the docking model*

The design and syntheses of novel nNOS inhibitors have been reported previously (21,22). In addition, the crystal structure of nNOS complexed with several of these, including cpd8, has been determined (11). Among them, we have chosen eight compounds representing a varied range of structure and activities (summarized in Table 1).

### *Statistical analysis*

Data are presented as the mean ± SD and Student's *t*-test was used to compare two groups, with a $p$ value of $<0.05$ considered statistically significant. All tests were two sided. One-way Analysis of Variance was performed to study the association between the nNOS staining scores and disease stages, followed by linear trend analysis. Linear regression analysis was applied to study the association between nNOS/iNOS inhibition and anti-invasion activities of novel synthesized inhibitors. The coefficient of determination ($R^2$) and the $p$-value were reported.

## Acknowledgments

The authors sincerely thank Drs. Glenn Merlino and Raza Zaidi (Laboratory of Cancer Biology & Genetics, National Cancer Institute, National Institutes of Health) for generously providing mouse melanoma cell lines and primary mouse melanocytes and Dr. M. Herlyn for generously providing wm3211 and Lu1205 human melanoma cells. We thank Drs. Daniel Gillen and Wen-pin Chen (Biostatistician, UC Irvine) for their assistance with the statistical analysis. Our thanks also go to Alisz Demecs for her diligent editorial assistance.

This work was supported primarily by a seed grant from the Chao Family Comprehensive Cancer Center (Ca62230 to S. Yang). The authors are grateful to the National Institutes of Health for financial support (GM49725 to R. Silverman and GM57353 to T. Poulos).

## Author Disclosure Statement

No competing financial interests exist.

## References

1. Ahmad N, Srivastava RC, Agarwal R, and Mukhtar H. Nitric oxide synthase and skin tumor promotion. *Biochem Biophys Res Commun* 232: 328–331, 1997.
2. Ahmed B, and Van Den Oord JJ. Expression of the neuronal isoform of nitric oxide synthase (nNOS) and its inhibitor, protein inhibitor of nNOS, in pigment cell lesions of the skin. *Br J Dermatol* 141: 12–19, 1999.
3. Ahmed B, and Van Den Oord JJ. Expression of the inducible isoform of nitric oxide synthase in pigment cell lesions of the skin. *Br J Dermatol* 142: 432–440, 2000.
4. Autier P, Dore JF, Eggermont AMM, and Coebergh JW. Epidemiological evidence that UVA radiation is involved in the genesis of cutaneous melanoma. *Curr Opin Oncol* 23: 189–196, 2011.
5. Berking C, Takemoto R, Satyamoorthy K, Elenitsas R, and Herlyn M. Basic fibroblast growth factor and ultraviolet B transform melanocytes in human skin. *Am J Pathol* 158: 943–953, 2001.
6. Burnett ME, and Wang SQ. Current sunscreen controversies: a critical review. *Photodermatol Photoimmunol Photomed* 27: 58–67, 2011.
7. Chung CY, Madhunapantula SV, Desai D, Amin S, and Robertson GP. Melanoma prevention using topical PBISe. *Cancer Prev Res (Phila)* 4: 935–948, 2011.
8. Cichocki M, Blumczynska J, and Baer-Dubowska W. Naturally occurring phenolic acids inhibit 12-O-tetradecanoylphorbol-13-acetate induced NF-kappaB, iNOS and COX-2 activation in mouse epidermis. *Toxicology* 268: 118–124, 2010.
9. Crane BR, Arvai AS, Gachhui R, Wu C, Ghosh DK, Getzoff ED, Stuehr DJ, and Tainer JA. The structure of nitric oxide synthase oxygenase domain and inhibitor complexes. *Science* 278: 425–431, 1997.
10. De Fabo EC, Noonan FP, Fears T, and Merlino G. Ultraviolet B but not ultraviolet A radiation initiates melanoma. *Cancer Res* 64: 6372–6376, 2004.
11. Delker SL, Ji H, Li H, Jamal J, Fang J, Xue F, Silverman RB, and Poulos TL. Unexpected binding modes of nitric oxide

synthase inhibitors effective in the prevention of a cerebral palsy phenotype in an animal model. *J Am Chem Soc* 132: 5437–5442, 2010.
12. Dupin E, and Le Douarin NM. Development of melanocyte precursors from the vertebrate neural crest. *Oncogene* 22: 3016–3023, 2003.
13. Ekmekcioglu S, Ellerhorst JA, Prieto VG, Johnson MM, Broemeling LD, and Grimm EA. Tumor iNOS predicts poor survival for stage III melanoma patients. *Int J Cancer* 119: 861–866, 2006.
14. This reference has been deleted.
15. Gonzalez Maglio DH, Paz ML, Ferrari A, Weill FS, Czerniczyniec A, Leoni J, and Bustamante J. Skin damage and mitochondrial dysfunction after acute ultraviolet B irradiation: relationship with nitric oxide production. *Photodermatol Photoimmunol Photomed* 21: 311–317, 2005.
16. Grimm EA, Ellerhorst J, Tang CH, and Ekmekcioglu S. Constitutive intracellular production of iNOS and NO in human melanoma: possible role in regulation of growth and resistance to apoptosis. *Nitric Oxide* 19: 133–137, 2008.
17. This reference has been deleted.
18. This reference has been deleted.
19. Heller A. The need for monitoring the actual nitric oxide concentration in tumors. *Bioanal Rev* 1: 3–6, 2009.
20. Herlyn M, Hsu MY, Meier FE, Nesbit M, Hsu JY, Van Belle P, and Elder DE. E-cadherin expression in melanoma cells restores keratinocyte-mediated growth control and down-regulates expression of invasion-related adhesion receptors. *Am J Pathol* 156: 1515–1525, 2000.
21. Ji H, Delker SL, Li H, Martasek P, Roman LJ, Poulos TL, and Silverman RB. Exploration of the active site of neuronal nitric oxide synthase by the design and synthesis of pyrrolidinomethyl 2-aminopyridine derivatives. *J Med Chem* 53: 7804–7824, 2010.
22. Ji H, Li H, Martasek P, Roman LJ, Poulos TL, and Silverman RB. Discovery of highly potent and selective inhibitors of neuronal nitric oxide synthase by fragment hopping. *J Med Chem* 52: 779–797, 2009.
23. Ji H, Tan S, Igarashi J, Li H, Derrick M, Martasek P, Roman LJ, Vasquez-Vivar J, Poulos TL, and Silverman RB. Selective neuronal nitric oxide synthase inhibitors and the prevention of cerebral palsy. *Ann Neurol* 65: 209–217, 2009.
24. Johansson CC, Egyhazi S, Masucci G, Harlin H, Mougiakakos D, Poschke I, Nilsson B, Garberg L, Tuominen R, Linden D, Stolt MF, Hansson J, and Kiessling R. Prognostic significance of tumor iNOS and COX-2 in stage III malignant cutaneous melanoma. *Cancer Immunol Immunother* 58: 1085–1094, 2009.
25. Joshi M, and White WL. A radial growth phase human melanoma cell line and tumorigenic variants of the same cell line differentially express neuronal nitric oxide synthase. *J Invest Dermatol* 106: 290–290, 1996.
26. Knowles RG, and Moncada S. Nitric oxide synthases in mammals. *Biochem J* 298 (Pt 2): 249–258, 1994.
27. Leung EL, Fraser M, Fiscus RR, and Tsang BK. Cisplatin alters nitric oxide synthase levels in human ovarian cancer cells: involvement in p53 regulation and cisplatin resistance. *Br J Cancer* 98: 1803–1809, 2008.
28. Li C, Hu Z, Liu Z, Wang LE, Gershenwald JE, Lee JE, Prieto VG, Duvic M, Grimm EA, and Wei Q. Polymorphisms of the neuronal and inducible nitric oxide synthase genes and the risk of cutaneous melanoma: a case-control study. *Cancer* 109: 1570–1578, 2007.
29. Liebmann J, Kolb-Bachofen V, Mahotka C, and Suschek CV. Photolytically generated nitric oxide inhibits caspase activity and results in AIF-mediated cell death. *J Mol Med* 88: 279–287, 2010.
30. Lin JK, and Lin-Shiau SY. Mechanisms of cancer chemoprevention by curcumin. *Proc Natl Sci Counc Repub China B* 25: 59–66, 2001.
31. Liu W, and Wu S. Differential roles of nitric oxide synthases in regulation of ultraviolet B light-induced apoptosis. *Nitric Oxide* 23: 199–205, 2010.
32. Madhunapantula SV, Desai D, Sharma A, Huh SJ, Amin S, and Robertson GP. PBISe, a novel selenium-containing drug for the treatment of malignant melanoma. *Mol Cancer Ther* 7: 1297–1308, 2008.
33. Maksimovic-Ivanic D, Mijatovic S, Harhaji L, Miljkovic D, Dabideen D, Fan Cheng K, Mangano K, Malaponte G, Al-Abed Y, Libra M, Garotta G, Nicoletti F, and Stosic-Grujicic S. Anticancer properties of the novel nitric oxide-donating compound (S,R)-3-phenyl-4,5-dihydro-5-isoxazole acetic acid-nitric oxide *in vitro* and *in vivo*. *Mol Cancer Ther* 7: 510–520, 2008.
34. Martinez-Ruiz A, Cadenas S, and Lamas S. Nitric oxide signaling: classical, less classical, and nonclassical mechanisms. *Free Radic Biol Med* 51: 17–29, 2011.
35. Massi D, De Nisi MC, Franchi A, Mourmouras V, Baroni G, Panelos J, Santucci M, and Miracco C. Inducible nitric oxide synthase expression in melanoma: implications in lymphangiogenesis. *Mod Pathol* 22: 21–30, 2009.
36. This reference has been deleted.
37. This reference has been deleted.
38. Menter J, Nokkaew C, Sprewell A, Eatman D, and Harris-Hooker S. Pigment melanin mediates a redox reaction between adsorbed nitric oxide and O-2 *in vitro*. *Pigment Cell Melanoma Res* 24: 794–794, 2011.
39. Meyskens FL, Jr., and Berwick M. UV or not UV: metals are the answer. *Cancer Epidemiol Biomarkers Prev* 17: 268–270, 2008.
40. Mitchell D, Paniker L, Sanchez G, Trono D, and Nairn R. The etiology of sunlight-induced melanoma in Xiphophorus hybrid fish. *Mol Carcinog* 46: 679–684, 2007.
41. Mitchell DL, Fernandez AA, Nairn RS, Garcia R, Paniker L, Trono D, Thames HD, and Gimenez-Conti I. Ultraviolet A does not induce melanomas in a Xiphophorus hybrid fish model. *Proc Natl Acad Sci U S A* 107: 9329–9334, 2010.
42. Moore WM, Webber RK, Jerome GM, Tjoeng FS, Misko TP, and Currie MG. L-N6-(1-iminoethyl)lysine: a selective inhibitor of inducible nitric oxide synthase. *J Med Chem* 37: 3886–3888, 1994.
43. Noonan FP, Otsuka T, Bang S, Anver MR, and Merlino G. Accelerated ultraviolet radiation-induced carcinogenesis in hepatocyte growth factor/scatter factor transgenic mice. *Cancer Res* 60: 3738–3743, 2000.
44. Ohshima H, Sawa T, and Akaike T. 8-Nitroguanine, a product of nitrative DNA damage caused by reactive nitrogen species: formation, occurrence, and implications in inflammation and carcinogenesis. *Antioxid Redox Signal* 8: 1033–1045, 2006.
45. Oliveira CJ, Curcio MF, Moraes MS, Tsujita M, Travassos LR, Stern A, and Monteiro HP. The low molecular weight S-nitrosothiol, S-nitroso-N-acetylpenicillamine, promotes cell cycle progression in rabbit aortic endothelial cells. *Nitric Oxide* 18: 241–255, 2008.
46. Patel JB, Shah FD, Shukla SN, Shah PM, and Patel PS. Role of nitric oxide and antioxidant enzymes in the pathogenesis of oral cancer. *J Cancer Res Ther* 5: 247–253, 2009.
47. Romero-Graillet C, Aberdam E, Clement M, Ortonne JP, and Ballotti R. Nitric oxide produced by ultraviolet-irradiated

keratinocytes stimulates melanogenesis. *J Clin Invest* 99: 635–642, 1997.
48. Russo PA, and Halliday GM. Inhibition of nitric oxide and reactive oxygen species production improves the ability of a sunscreen to protect from sunburn, immunosuppression and photocarcinogenesis. *Br J Dermatol* 155: 408–415, 2006.
49. Savaraj N, You M, Wu C, Wangpaichitr M, Kuo MT, and Feun LG. Arginine deprivation, autophagy, apoptosis (AAA) for the treatment of melanoma. *Curr Mol Med* 10: 405–412, 2010.
50. Siegel R, Desantis C, Virgo K, Stein K, Mariotto A, Smith T, Cooper D, Gansler T, Lerro C, Fedewa S, Lin C, Leach C, Cannady RS, Cho H, Scoppa S, Hachey M, Kirch R, Jemal A, and Ward E. Cancer treatment and survivorship statistics, 2012. *CA Cancer J Clin* 62: 220–241, 2012.
51. Sikora AG, Gelbard A, Davies MA, Sano D, Ekmekcioglu S, Kwon J, Hailemichael Y, Jayaraman P, Myers JN, Grimm EA, and Overwijk WW. Targeted inhibition of inducible nitric oxide synthase inhibits growth of human melanoma *in vivo* and synergizes with chemotherapy. *Clin Cancer Res* 16: 1834–1844, 2010.
52. Silverman RB. Design of selective neuronal nitric oxide synthase inhibitors for the prevention and treatment of neurodegenerative diseases. *Acc Chem Res* 42: 439–451, 2009.
53. Szekeres T, Saiko P, Fritzer-Szekeres M, Djavan B, and Jager W. Chemopreventive effects of resveratrol and resveratrol derivatives. *Ann N Y Acad Sci* 1215: 89–95, 2011.
54. Tew KD, Manevich Y, Grek C, Xiong Y, Uys J, and Townsend DM. The role of glutathione S-transferase P in signaling pathways and S-glutathionylation in cancer. *Free Radic Biol Med* 51: 299–313, 2011.
55. Thomas DD, Ridnour LA, Isenberg JS, Flores-Santana W, Switzer CH, Donzelli S, Hussain P, Vecoli C, Paolocci N, Ambs S, Colton CA, Harris CC, Roberts DD, and Wink DA. The chemical biology of nitric oxide: implications in cellular signaling. *Free Radic Biol Med* 45: 18–31, 2008.
56. Tschugguel W, Pustelnik T, Lass H, Mildner M, Weninger W, Schneeberger C, Jansen B, Tschachler E, Waldhor T, Huber JC, and Pehamberger H. Inducible nitric oxide synthase (iNOS) expression may predict distant metastasis in human melanoma. *Br J Cancer* 79: 1609–1612, 1999.
57. Yang S, Irani K, Heffron SE, Jurnak F, and Meyskens FL, Jr. Alterations in the expression of the apurinic/apyrimidinic endonuclease-1/redox factor-1 (APE/Ref-1) in human melanoma and identification of the therapeutic potential of resveratrol as an APE/Ref-1 inhibitor. *Mol Cancer Ther* 4: 1923–1935, 2005.
58. Yang S, McNulty S, and Meyskens FL, Jr. During human melanoma progression AP-1 binding pairs are altered with loss of c-Jun *in vitro*. *Pigment Cell Res* 17: 74–83, 2004.
59. Yang S, Misner BJ, Chiu RJ, and Meyskens FL, Jr. Redox effector factor-1, combined with reactive oxygen species, plays an important role in the transformation of JB6 cells. *Carcinogenesis* 28: 2382–2390, 2007.
60. Yang TS, Lu SN, Chao Y, Sheen IS, Lin CC, Wang TE, Chen SC, Wang JH, Liao LY, Thomson JA, Wang-Peng J, Chen PJ, and Chen LT. A randomised phase II study of pegylated arginine deiminase (ADI-PEG 20) in Asian advanced hepatocellular carcinoma patients. *Br J Cancer* 103: 954–960, 2010.
61. Yang Z, Yang S, Misner BJ, Chiu R, Liu F, and Meyskens FL, Jr. Nitric oxide initiates progression of human melanoma via a feedback loop mediated by apurinic/apyrimidinic endonuclease-1/redox factor-1, which is inhibited by resveratrol. *Mol Cancer Ther* 7: 3751–3760, 2008.

Address correspondence to:
*Dr. Sun Yang*
*Chao Family Comprehensive Cancer Center*
*University of California Irvine*
*B200 Sprague Hall*
*Irvine, CA 92697*

*E-mail:* syang2@uci.edu

Date of first submission to ARS Central, February 10, 2012; date of final revised submission, November 07, 2012; date of acceptance, December 01, 2012.

**Abbreviations Used**

APE/Ref-1 = apurinic (apyrimidinic) endonuclease/redox-factor 1
CM = cutaneous melanoma
DETA NONOate (DETA/NO) = (Z)-1-[2-(2-aminoethyl)-*N*-(2-ammonioethyl) amino] diazen-1-ium-1,2-diolate
DMEM = Dulbecco's Modified Eagle Medium
eNOS = endothelial NOS
FBS = fetal bovine serum
HGF/SF = hepatocyte growth factor/scatter factor
IHC = immunohistochemistry
iNOS = inducible NOS
MTT = 3-(4,5-dimethylthiazol-2-yl)-2,5-diphenyltetrazolium bromide
nNOS = neuronal NOS
NO = nitric oxide
NOS = nitric oxide synthase
PBS = phosphate-buffered saline
ROS = reactive oxygen species
siRNA = small interfering RNA
SOD = superoxide dismutase
ST = Spermidine trihydrochloride
UV = ultraviolet